Improved Efficiency of the Microwave Enhanced Catalytic Pyrolysis of Methane, Through Supplemental Thermal Heating

Troy Christiansen[+], Brandon Robinson[+], Ashley Caiola, Changle Jiang, and Jianli Hu[*].

Department of Chemical & Biomedical Engineering, West Virginia University, Morgantown, WV 26506, U.S.A.

*Corresponding author E-mail: john.hu@mail.wvu.edu

+ T. Christiansen and B. Robinson are equal contributors

Abstract:

Methane catalytic pyrolysis is a promising solution for producing hydrogen and valuable carbon nanotubes (CNTs) from natural gas without the production of CO_2 emissions. The microwave-enhanced methane catalytic pyrolysis was conducted in a hybrid fixed bed reactor that allows for microwave heating and combined thermal microwave "hybrid" heating experiments. In the hybrid heating mode, the catalyst was heated to a temperature of 500°C with hot air, and then the catalyst temperature was raised to the operating temperature utilizing microwave irradiation. The Ni-Pd/CNT catalyst was tested at 550-650°C under hybrid or microwave-only conditions. Hybrid heating was found to have a higher methane conversion than microwave heating alone. The higher conversion was attributed to the more efficient utilization of the catalyst bed and temperature uniformity, as indicated by the thermal imaging results. The power required to maintain the reaction temperature was reduced in the hybrid heating mode by over 60% of what was initially needed under microwave heating only. XRD, Raman, TGA, and TEM were used to characterize the morphology of the carbon nanotube product formed. The CNTs formed were found to be more uniform under hybrid heating than microwave heating alone, indicated by TGA oxidation temperatures. This work demonstrates the potential of utilizing industrial waste heat to lower the overall size of the microwave generator, increase catalyst utilization, and reduce input energy requirements, thus lowering capital and energy costs.

1.0 Introduction

The combustion of fossil fuels for heat and electricity has become an essential part of our global society while, at the same time, unmitigated carbon emissions are threatening the population. Hydrogen is a critical alternative energy fuel for supporting a decarbonized world. [1] Hydrogen production from methane is performed via two main chemical processes, steam reforming (SMR) and pyrolysis. Currently, SMR is the most economically suitable technology for hydrogen production from methane, which accounts for 90% of the global hydrogen supply. However, its disadvantage is the inevitable carbon dioxide production via the water-gas shift reaction. [2][3] The pairing of carbon capture and sequestration (CC&S) with SMR could reduce the CO_2 emissions at an added cost for CC&S. Another disadvantage of SMR is its high operating pressures which drive the high capital costs.

Hydrogen produced through methane catalytic pyrolysis (MCP) is one of the promising technological paths for producing CO_2-free hydrogen. [4][5][6][7] MCP converts methane over a solid catalyst into hydrogen gas and solid carbon, as seen in Equation 1. The conversion of methane to hydrogen reduces the fuel value by 35%, and the carbon produced from MCP is of low-value carbon black. MCP industrial processes suffer from low-profit margins and rely heavily on process efficiency and carbon product market value. Recently, attention has been drawn to MCP, focusing on creating higher-value carbon products to overcome the economic hurdles associated with MCP applications.

$$CH_4 = C_{(solid)} + 2H_2 \quad (1)$$

Carbon nanotubes are a carbon product that could significantly improve the profit margins for MCP industrial processes. Carbon nanotube-producing MCP catalytic enhancements have been focused mainly on metal-support interactions [8]–[12], where metal leaching from the support is a significant issue of catalyst deactivation.[13] A catalyst selective to base-grown carbon nanotubes prevented metal leaching by leaving the metal attached to the catalyst support and not connected to the carbon nanotube product tip. The MCP process's separation of CNTs from the catalyst support is a significant challenge. Mechanical separation by attrition in a fluidized-bed reactor system resulted in a poor separation efficiency of CNTs from the support.[14] A Ni-Pd/CNT catalyst was tested in our recent study under cyclic reaction-regeneration experiments. An acid treatment method was demonstrated to recover catalyst metals from the tip and base-grown CNTs.[15] The Ni-Pd/CNT catalyst was regenerated, and a portion of the CNT product was re-applied as the new catalyst support and re-doped with the Ni-Pd dissolved metals. The process was determined to be self-sustained without the need for additional external catalyst metals or CNTs. Density functional theory was also used to understand MCP's fundamental reaction pathways over the Ni-Pd/CNT catalyst. [15], [16]

Microwave heating for heterogeneous catalysis offers advantages over conventional heating systems. Selective heating, the heating of materials based on their ability to absorb and convert

microwave radiation into heat, and volumetric heating, eliminates radial heat gradients as the whole volume of the catalyst bed is heated without relying on conduction. These advantages help perform methane decomposition as the methane and hydrogen gas phase does not appreciably absorb microwaves in their normal state. Previously, our group studied the effects of microwave heating on MCP and compared it to conventional thermal heating over the Ni-Pd/CNT catalyst.[17] The microwave heating mechanism of the catalyst studied combines the joule-heating of the CNT support and dielectric heating of the metal nanoparticles.[18][19] The presence of free electrons in the carbon atoms within the CNT enables the CNT support to absorb microwave irradiation effectively and turn it into heat energy. It was determined that the microwave-enhanced MCP showed improvements in kinetics, where the apparent activation energy dropped from 45.5 kJ/mol under conventional heating to 24.8 kJ/mol under microwave irradiation. Process simulation and techno-economic analysis showed that a possible hydrogen minimum selling price of $1kg/H2 could be achieved.

In this work, the performance of a Ni-Pd/CNT catalyst was tested under a hybrid thermal-microwave heating system and compared to microwave heating alone. The proposed combined thermal-microwave heating system seeks to alleviate the issues with thermal or microwave heating techniques. It is thought that additional external heat can lower required microwave input energy and increase the catalyst bed temperature homogeneously, thus improving selectivity and conversion. The research objective is to demonstrate the potential of transforming natural gas into clean hydrogen and value-added carbon in a more energy-efficient way than thermal heating alone by utilizing microwave irradiation and industrial waste heat.

2.0 Experimental

Catalyst Synthesis. A bimetallic catalyst containing 11 wt.% Ni/Pd with a ratio of 10:1 Ni:Pd was prepared using as-dispersed, size-controlled nanoparticles of 10-30 nm supported on carbon nanotubes synthesized using a solvothermal process.[15] Nickel nitrate hexahydrate and palladium nitrate dihydrate were procured from Acros Organics and Sigma-Aldrich. Dry 20-30 nm diameter 10-30 μm in length multiwalled carbon nanotubes procured from Cheap Tubes were added to the metal precursors solution under stirring until well mixed. The precursors were dissolved in 50 ml of acetone under stirring until fully dissolved. The metal precursor and nanotube solution were then sonicated for 30 mins while minimizing evaporation. The sonicated mixture was then transferred to a Teflon-lined autoclave and placed in an oven set to 120°C for 12 hours. The autoclave was then removed from the oven and allowed to cool to room temperature. The produced solution was then dried in air for 12 hours at 80°C. The prepared Ni-Pd/CNT catalyst was pulverized in a mortar and pestle until a fine powder was produced. The catalyst was then reduced in a hydrogen/nitrogen environment in a tube furnace set to 600°C for 4 hours.

CNT Characterization. Oxidative-thermogravimetric analysis (TGA) was carried out in a TA-Instruments SDT-650. The unreacted catalyst, reacted catalysts, and the additional standard mixtures of the prepared catalyst, CNTs, and carbon black were also analyzed. These standards highlight the differences in the oxidation rate of amorphous and crystalline carbon. The samples

were oxidated in a 50/50 mixture of nitrogen and air at a total flow rate of 200 sccm. The temperature was raised from 50°C to 400°C at a rate of 10°C/min and held at 400°C for 30 minutes. Then the temperature was raised further from 400°C to 700°C at 2°C/min. Transmission electron microscopy (TEM) was conducted using a JEOL TEM 2100 electron microscope operating at 200 kV. Images of the prepared catalyst and reacted catalysts were obtained, showing the size of the attached Ni/Pd nanoparticles and the morphology and size of the produced carbon products. The samples were sonicated in acetone for 10 minutes before loading onto a copper mesh grid coated with a formvar film.ImageJ software was used to measure the nanoparticle diameters by counting the linear pixels with the known pixel length corresponding to the resolution and displayed scale. Several images were used with care not to double-count. X-ray diffraction (XRD) was carried out on a Panalytical X'pert Pro from 10° 2θ to 90° 2θ at 45Kv using a rotating stage setup. The CNT catalyst was loaded into an XRD slide with the top prepared as flat as possible. Raman spectroscopy was performed using a Renishaw InVia Raman Microscope using a 532 nm laser at 10 mW. The spectra were accumulated 3 times with an exposure time of 10 seconds each.

Microwave and Hybrid Reactor. The catalyst was evaluated for methane pyrolysis under a combined thermal-microwave system. The setup can be seen in Figure 1, where a 900-watt 2.45 GHz Sairem GMS1000 solid-state generator, complete with an automatic 4-stub tuner, was used to supply microwave irradiation with minimal reflected power. Concentric quartz tubes of 12mm-ODx10mm-ID and 24mm-ODx20mm-ID were placed in the center of a mono-mode high-temperature microwave cavity. 0.2 grams of catalyst was loaded into the 10mm-ID tube supported by quartz wool. The catalyst was heated to operating temperature under 50 sccm of nitrogen in both MW only and Hybrid heating modes. In hybrid heating mode, the catalyst bed was thermally preheated to 500°C by a SureHeat jet heater with an airflow rate of 8 scfm through the concentric quartz tubes. The catalyst bed was then raised from 500°C to the selected operating temperatures of 550°C, 600°C, and 650°C under microwave irradiation. In microwave-only mode, the catalyst was heated by microwave irradiation to reaction temperature at a 10°C/min rate to the corresponding temperature. Once reaction temperatures was reached, the gas flow was changed to 40 sccm methane and 10 sccm nitrogen. The mass of the catalyst was recorded before and after the reaction. The reaction product gas was analyzed with a ThermoScientific Mass Spectrometer Prima BT. The catalyst bed temperature was controlled by a short-wave infrared Micro-Epsilon pyrometer model CTM-3SF75H1-C3 set to an emissivity value of 0.80. Infrared images were recorded with a FLIR model A6261 short-wave infrared thermal image set to an emissivity value of 0.80. A factory-calibrated neutral density filter was installed for temperature measurements of 400-700°C. The camera was placed at a consistent distance of 0.5 meters from the catalyst bed resulting in a pixel resolution of 4 pixels per millimeter. The IR pyrometer was positioned 2" from the vertically oriented catalyst bed. The thermal imager was directly oriented at the opposite side of the vertically aligned catalyst bed. Together, the thermal imager and the IR pyrometer spot size cover nearly 70% of the external surface of the catalyst bed.

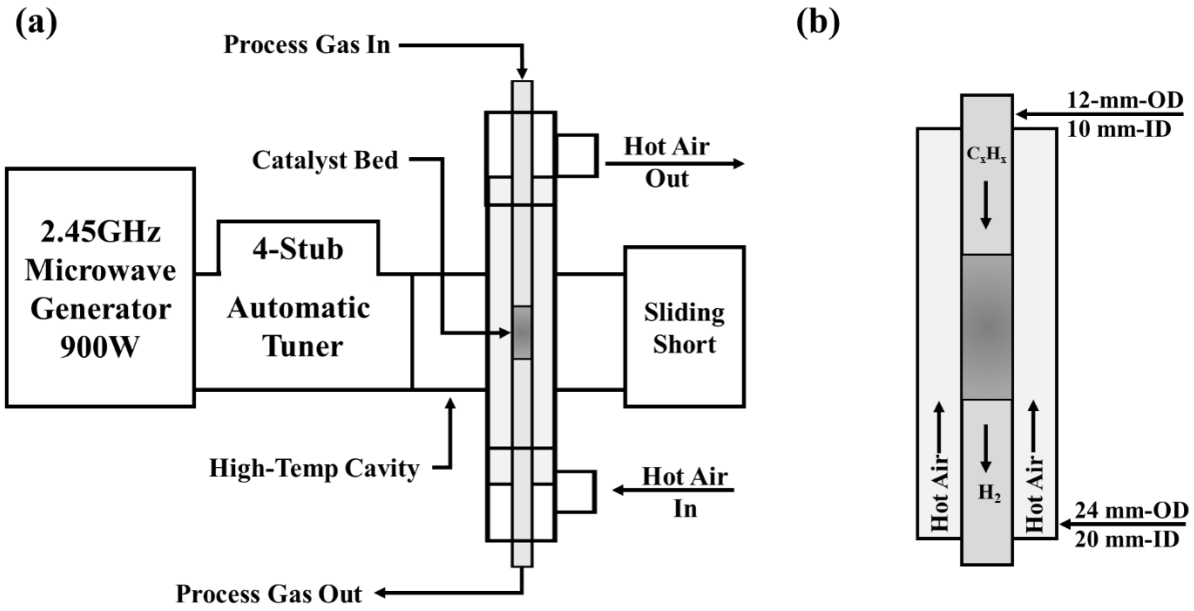

Figure 1: Diagram of the hybrid heating reactor setup where (a) is a generalized illustration of the microwave components and (b) is a generalized illustration of the catalyst bed in the cavity.

3.0 Result and Discussion

Performance of the Ni-Pd/CNT Catalyst. The 10Ni-1Pd/CNT catalyst was tested under microwave heating at three different temperatures of 550°C, 600°C, and 650°C. The microwave reactor directly heats the catalyst via joule heating of the CNT support and dielectric heating of the metal nanoparticles. This heating mechanism has been shown previously to improve the catalytic action compared to conventional heating by increasing the active site temperature while keeping the gas phase temperatures low.[17] As seen in Figure 2, the first-pass conversion of methane is approximately 50% at 550°C and 600°C, with a significantly lower conversion rate at 650°C. As the reaction temperature increases in microwave heating, the rate of deactivation increases, likely due to sintering or Ostwald ripening the metal nanoparticles into larger and less active particles. Due to temperature-dependent dielectric properties, a microwave absorption "runaway" can occur, leading to hotspot formation that absorbs more microwave radiation than the cold spots in the system. Higher temperatures accelerate this process as the microwave generator does not homogenously heat the catalyst, and hotspots form, causing deactivation.

The hybrid heating mode was thought to create a more uniform temperature distribution across the catalyst bed in comparison to the microwave-only mode of heating. At 550°C, the hybrid heating mode resulted in a slightly lower conversion than microwave heating alone. The more uniform heat distribution resulted in less intense hotspot regions, decreasing catalyst conversion. However, as the reaction temperature increased to 600°C and 650°C, the hybrid heating mode resulted in a higher conversion than microwave heating alone. With a higher conversion than microwave alone,

Hybrid-600°C and Hybrid-650°C demonstrate the importance of allowing for a difference in reaction temperature and the preheating temperatures allowing for hot spot formations.

Hybrid heating of the Ni-Pd/CNT catalyst improves several deficiencies of microwave heating alone. As seen in Figure 3a, the first improvement is the decrease in electrical energy required by the microwave generator to maintain the catalyst temperature under reaction conditions on a watt/gram basis. The microwave's power consumption was reduced from 85 watts of microwave power at 550°C under microwave irradiation to only 24 watts for the hybrid heating system. The hybrid heating mode also produced hydrogen more efficiently than microwave heating alone on an mg-hydrogen/ watt/gram catalyst basis, as seen in Figure 3b. Most of the process heat needed for the reaction was derived from the heat exchange of hot air to the catalyst bed. As the reaction temperature was increased, more microwave power was required to reach the higher reaction temperatures. The higher reaction temperatures led to faster catalyst deactivation, with the greatest yield measured at 600°C in hybrid mode. Hybrid heating dramatically reduces the electricity needed to perform microwave catalysis while improving catalyst productivity per watt of microwave irradiation. By utilizing industrial waste heat in scaled-up microwave reactor systems, the size and power of the system required could be significantly reduced, thus lowering the total capital cost and energy consumption.

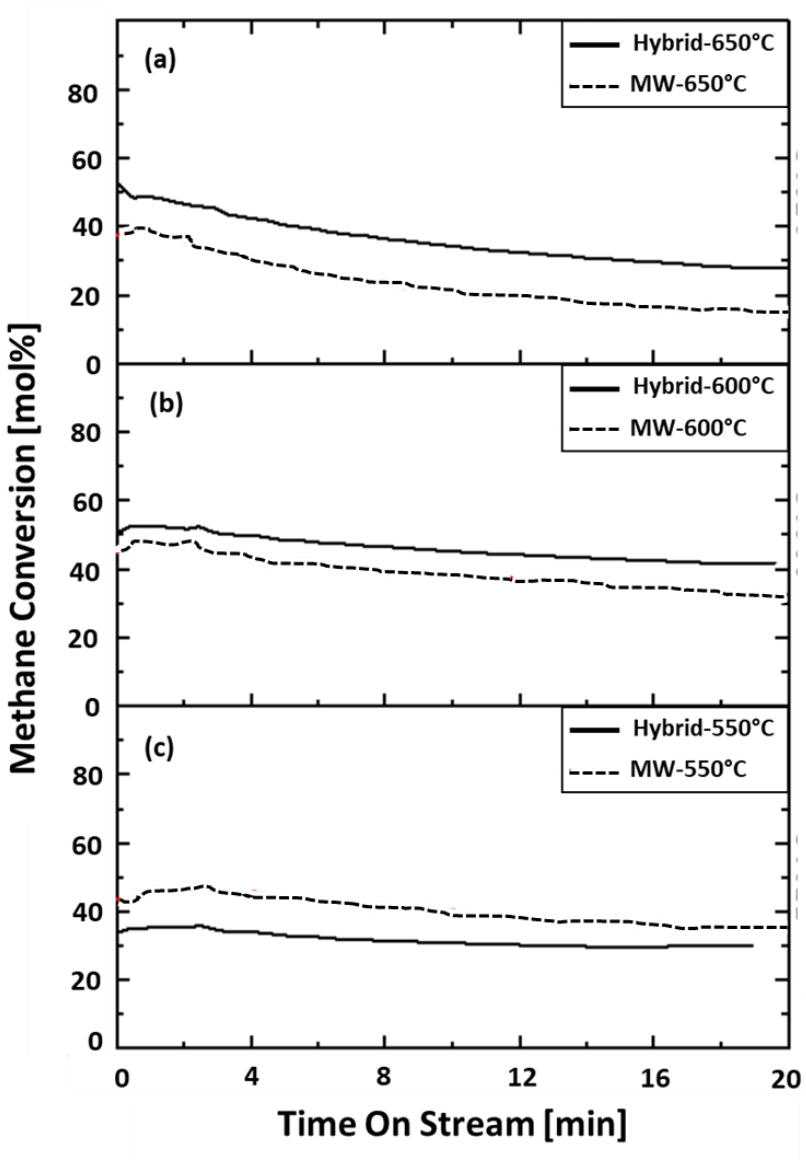

Figure 2: Conversion of methane at the defined reaction temperatures in the microwave and hybrid modes.

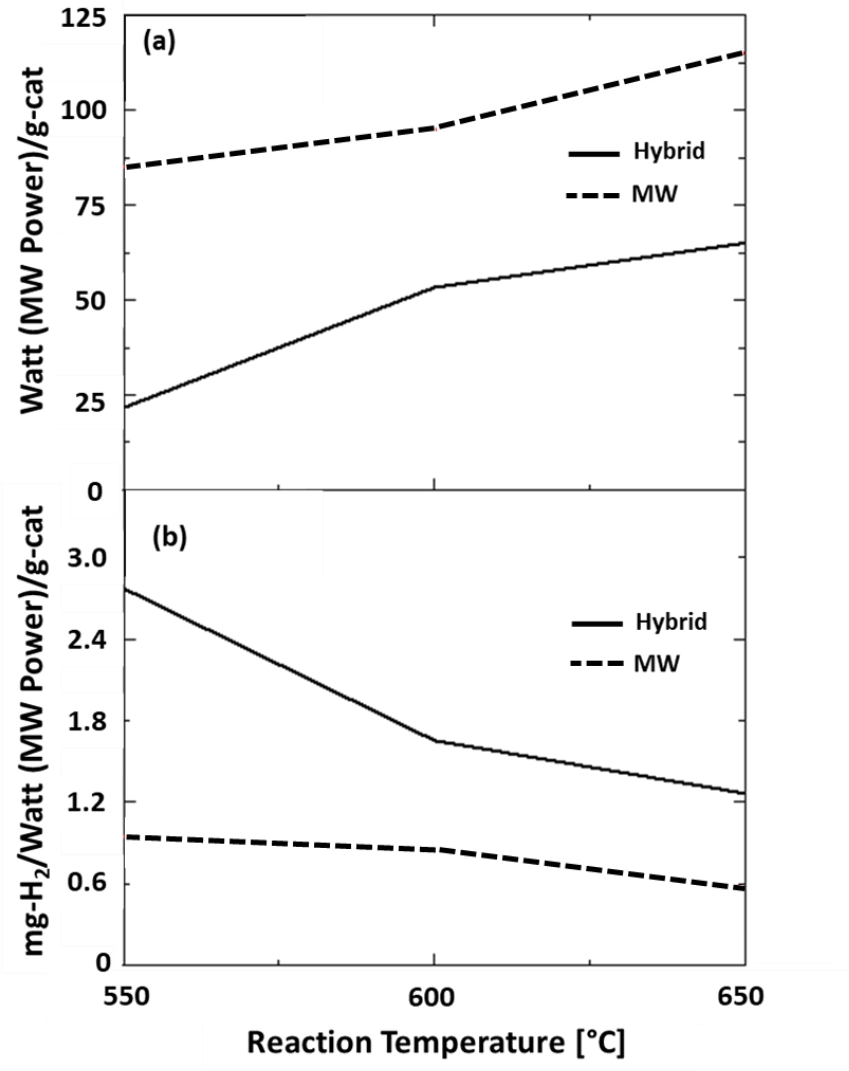

Figure 3: The microwave power consumption, (a) watt/gcat consumption, and (b) the production of hydrogen per watt of microwave power.

Temperature Distribution. The second improvement is the increase in catalyst bed utilization and a decrease in temperature variation across the catalyst bed. Figure 4, shows the histograms of the temperature distribution across the catalyst bed observed by a thermal imaging camera. Figure 4(a-b) illustrates the wide surface temperature distribution recorded by the infrared camera for the MW-550°C, Hybrid-550°C, and the preheated catalyst. The slight contradiction in the pyrometer and the thermal imagers' temperature distributions can be attributed to the orientation of the pyrometer in relation to the thermal imager. The pyrometer and the thermal imager are positioned facing opposite sides of the vertically oriented catalyst bed inside the reactor tube.

The MW-550°C temperature distribution, as seen in Figure 4c, had a wide distribution range with an average pixel surface temperature centered around 490°C. As seen in Figure 4b, the hot air

preheaters temperature distribution serves as a baseline temperature distribution for the hybrid heating method. The experimental setup produced a narrow surface temperature distribution centered around 510°C, which was held constant for all samples in the hybrid heating modes. The Hybrid-550°C produced a much more limited temperature distribution than MW-heating alone. The MW-650°C temperature distribution, as seen in Figure 4d, indicated that a hotspot had formed with a temperature centered around 680°C and a wide range of temperature measurements below the 650°C setpoint.

Hotspot formation and poor catalyst bed utilization were readily apparent in the MW heated catalysts, as indicated by the wide temperature distribution across the catalyst bed and off-temperature high pixel counts. The hotspot formations cause the temperature-dependent dielectric properties of the catalyst material and the presence of focused microwave irradiation. As the catalyst material is heated, the material's ability to absorb microwave irradiation changes, typically increasing with increasing temperatures.[20] It can also be seen in Figure 4, that the MW heated catalyst temperature distribution becomes more significant with increasing setpoint temperatures. This was attributed to increased heat losses from the catalyst bed resulting in higher excess cavity power. At the higher temperature setpoints, given its uninsulated cavity. The microwave also required more power to reach the setpoint temperature, thus amplifying the temperature inhomogeneity and the severity of the hotspot formed. Hotspot formation can significantly reduce the utilization of the catalyst bed and lead to accelerated deactivation at higher reaction temperatures.

Hybrid heating showed a more limited distribution and a higher temperature median than microwave heating alone for all reaction temperatures, as seen in Figure 4. The narrower temperature distribution across the catalyst bed was attributed to the hybrid heating's insulating nature, thus resulting in fewer overall thermal losses from the catalyst bed. The narrow temperature distribution indicates that a more efficient catalyst bed utilization was achieved. Using a hybrid heated reactor could mitigate the effects of hotspot formations, thus improving catalyst bed utilization and controllability of the bulk catalyst bed temperature. These effects are mitigated by the hybrid mode of heating, which reduces microwave power, thus decreasing the temperature difference between bulk temperatures and hotspot temperatures.

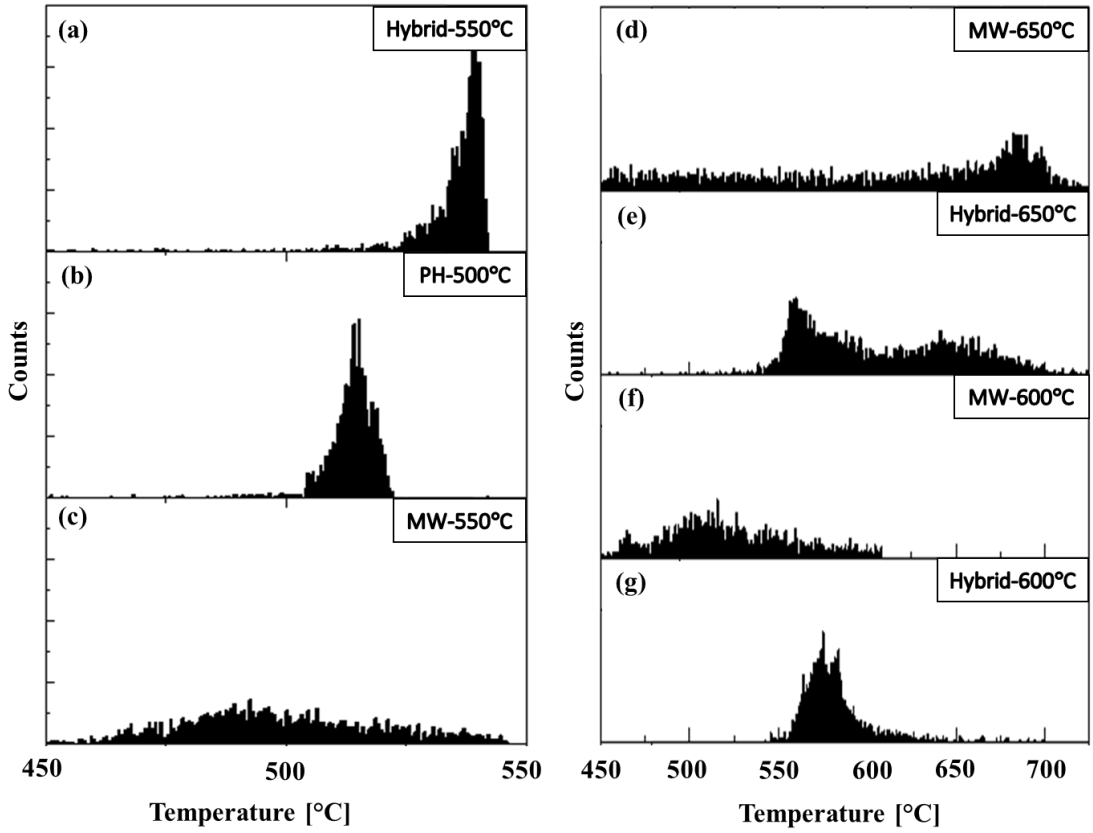

Figures 4. Catalyst temperature distributions of the (a) Hybrid-550°C, (b) Preheated Catalyst set to 510°C, (c) MW-550°C, (d) MW-650°C, (e) Hybrid-650°C, (f) MW-600°C, and (g) Hybrid-600°C.

X-Ray Diffraction. XRD of the catalyst was performed before and after the reaction under the specified heating method, as seen in Figure 5. The peaks at 26, 43, and 78 are characteristic of the CNT support. The minor peaks at 44, 54, and 76 present in the fresh catalyst indicate metallic nickel. The palladium is present in too small of an amount to be detectable above the instrument's noise at the particle size present in the catalyst. [21], [22] There is a significant reduction in the peak intensity of the metals at the lower reaction temperatures. This reduction in peak intensity is likely due to the greater sustained conversion, thus resulting in a higher overall yield at the lower reaction temperatures than the fast deactivation at 650°C. The decrease in the metal concentration or the formation of carbon covering the particles during the reaction obscures the metals' presence. However, at 650°C, there is no significant decrease in peak intensity, even with a yield only somewhat less than the lower reaction temperatures. This is due to sintering or Ostwald ripening of the metal particles during the reaction, thus increasing their size and appearance in the instrument.[23]

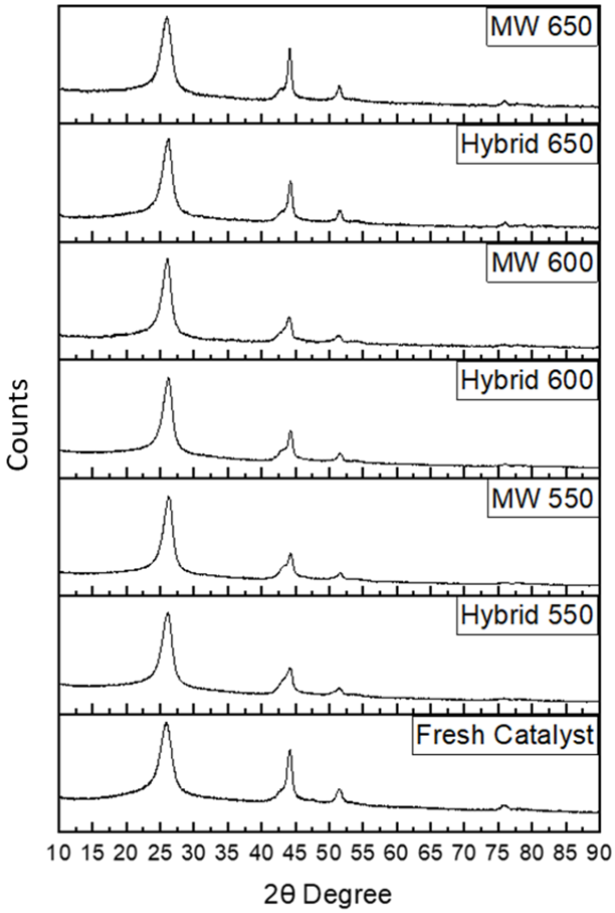

Figure 5: XRD spectra of the fresh catalyst compared to the reacted hybrid and microwave heated at 550°C, 600°C, and 650°C.

Thermogravimetric Analysis. The type of carbon produced was further characterized by thermogravimetric analysis in air, as seen in Figures 6 and 7. Standard samples, as seen in figure 6, are compared to the reacted samples in figure 7. In the amorphous and crystalline, carbon can be readily distinguished by oxidative thermogravimetric analysis.[24] The peaks of the 1st derivative show the oxidation of different phases of carbon. The less ordered amorphous carbon is typically oxidized at lower temperatures than the CNTs. In figure 7, it can be seen that the microwave and the hybrid heating modes both produce carbon that is consistent with the fresh CNTs oxidation temperature, as seen in figure 6b. The microwave and the hybrid spent samples, as seen in figure 7, show the lack of TGA weight loss within the amorphous carbon temperature range. The appearance of only one 1st derivative and the higher weight retention at 450°C indicates the carbon formed was of a higher order for the microwave and hybrid heating modes. The hybrid heating mode was observed to have an effect on the morphology of the coke produced as compared to the microwave-only heated sample upon closer inspection of the DTA signal. The microwave-heated sample produced a slightly broader DTA signal skewed towards higher oxidation

temperatures when compared to the hybrid heating mode. This shift to higher temperatures suggests that microwave-heated samples could have produced carbon that is more ordered in structure (multiwalled CNTS and Fibours CNTs) or carbon of graphitic nature. This suggests that hybrid heating can affect the morphology of the CNTs and improve the uniformity of the produced carbon.

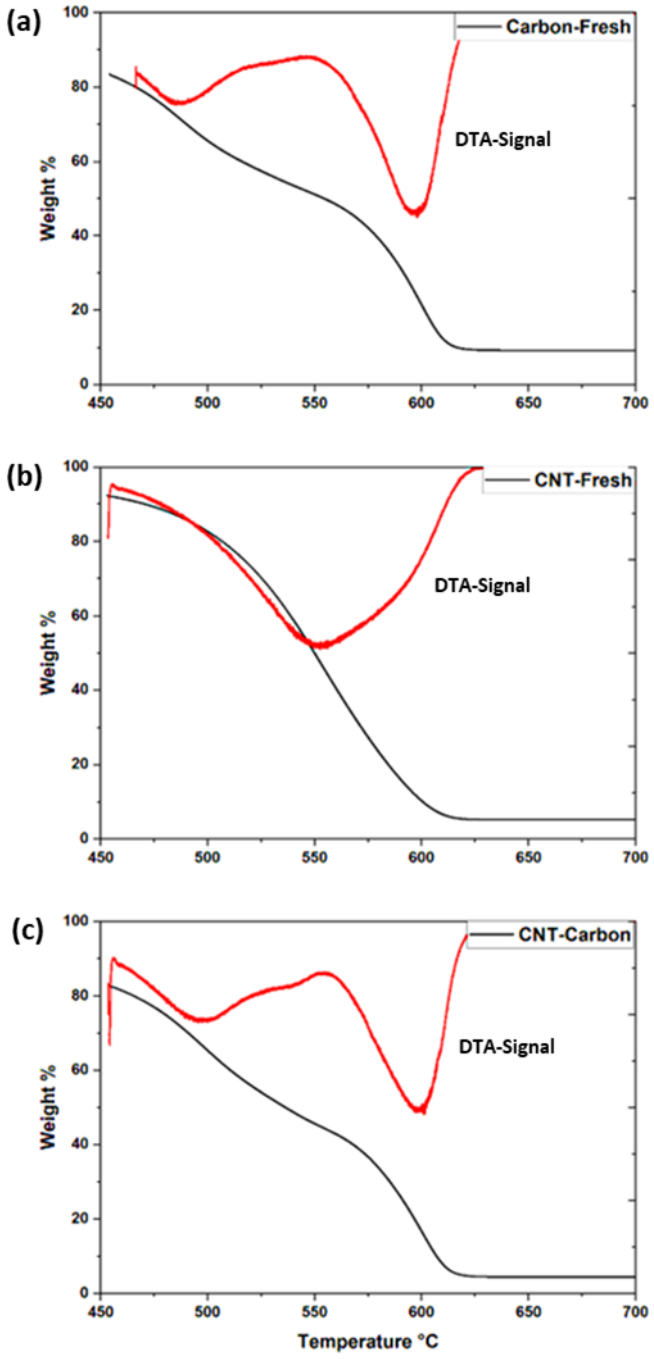

Figure 6: Oxidative TGA weight loss and rate of weight change for the standards (a) CNTs with carbon (b) carbon and unreacted catalyst, and (c) CNTs and unreacted catalyst..

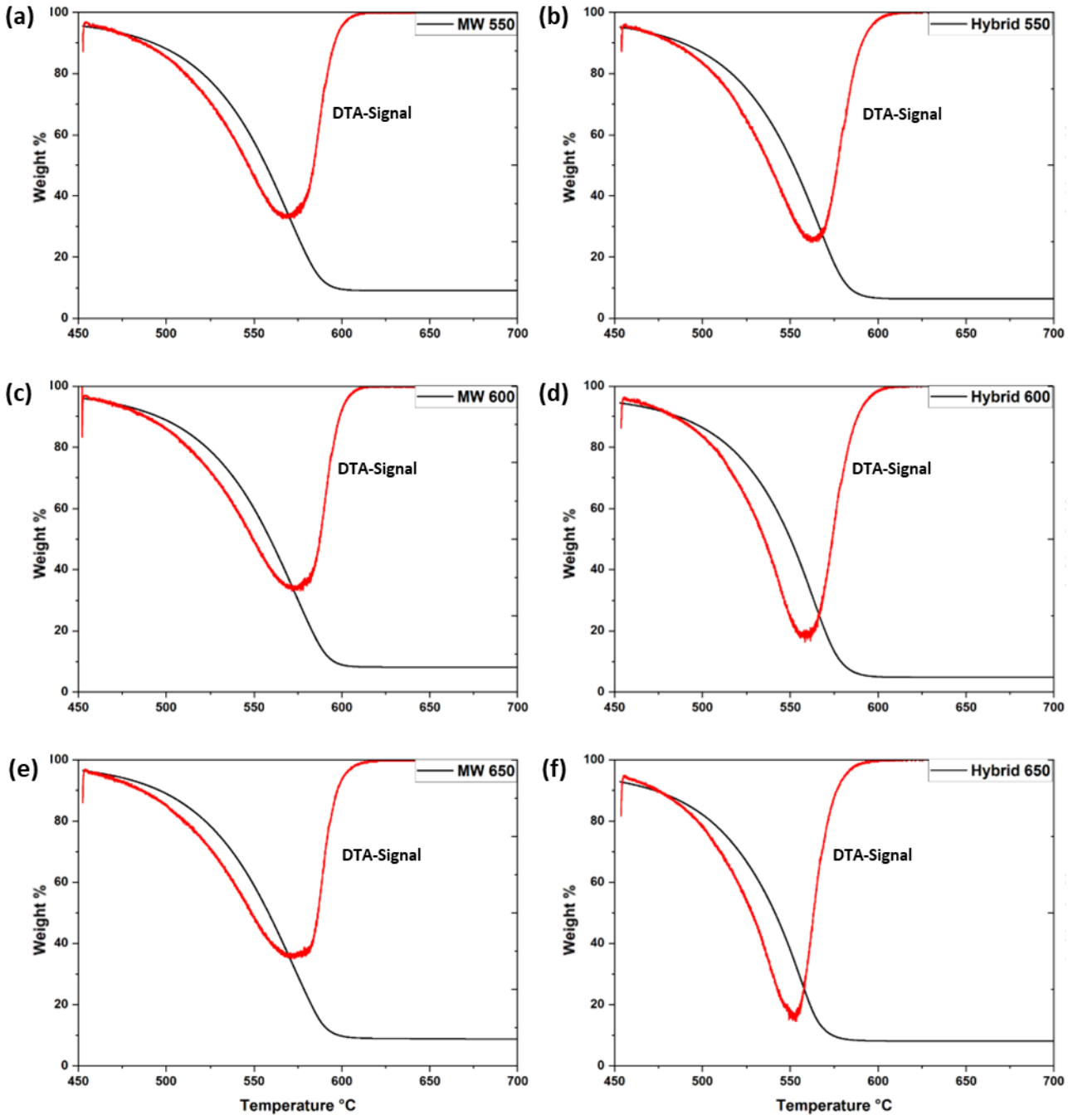

Figure 7: Oxidative TGA weight loss and rate of weight change for the reacted catalyst where (a) MW-550°C. (b) Hybrid-550°C. (c) MW-600°C. (d) Hybrid-600°C, (e) MW-650°C. and (f) MW-650°C.

Raman IR Analysis. The Raman spectra were collected to clarify the type of crystalline carbon formed on the sample during the reaction. The prominent peaks at 1350 and 1600 cm^{-1} and 2700 cm^{-1} indicate the presence of multiwalled carbon nanotubes (MWCNT). The small peak at 2450 cm^{-1} indicates no substantial graphite in the sample as no characteristic "hump" is centered on 2500

cm-1.[25] As seen in Figure 8, the TGA results and the Raman spectra confirm that the produced carbon is composed primarily of MWCNTs and not graphitic carbon.

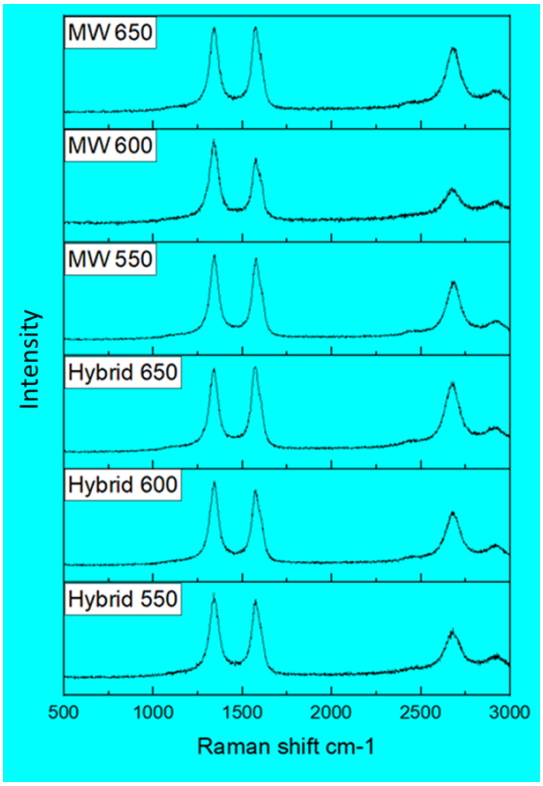

Figure 8: Raman spectra of the reacted catalysts under hybrid and microwave heating modes.

Carbon and Particle Morphology. TEM images of the bare CNTs and the as-prepared Ni-Pd/CNT catalyst with attached metal particles of different sizes are shown in Figure 9. Metal particle size has been shown to influence the morphology and selectivity of the produced carbon significantly.[25] It was found that smaller than 10nm particles resulted in quick deactivation due to graphite encapsulation. In contrast, larger particles reduce the number of active metal sites by weight and generate less ordered structures. Figure 10 shows the fresh catalyst particle size distribution; the fresh catalyst was found to have an average particle size distribution centered around 20 nm in diameter. The Hybrid-600°C catalyst is also shown in Figure 10, where the average particle size distribution shifted towards larger particles. It was found that the nanoparticles increased in size during the reaction compared to the unreacted catalyst. The hybrid and microwave-only modes produced a similar particle size distribution, as shown in Figure 11. Nanoparticle enlargement is a likely source of deactivation and may affect the morphology and size of the produced CNTs.

Identifying the growth method was obfuscated by the similarity of the support and the grown carbon. Still, through careful examination and knowledge of the as-synthesized attachment positions of the nanoparticles, identification of the grown CNTs was elucidated.

TEM Images of the reacted catalysts are shown in Figure 12 for the hybrid, and Figure 13 for the MW reacted catalysts. The frequent occurrence of nanoparticles with CNT growth still attached to the sides of the supporting CNTs indicates that tip growth was the primary mode of carbon growth during the reaction.[26] Evidence for this is the frequent occurrence of branching CNT growth on the supporting CNTs, as would be expected from tip growth. Another possibility is that due to the weak strength of the nanoparticles' attachment to the supporting CNTs, physical stresses may have sheared off the nanoparticles from the support, obscuring base growth. The observed nanoparticles were still attached to the supporting CNTs and did not have substantial carbon growth. Also, no CNTs outside the specified size range of the support were found without nanoparticles attached at the tip. Suppose an acid-wash catalyst separation process was employed, like the one developed in our lab.[13] In that case, the successive CNTs growing from the surface of the CNTs could result in tangled and interwoven meshes of CNTs that may have beneficial applications in composite materials as a nanoaggregate or as reinforcement.

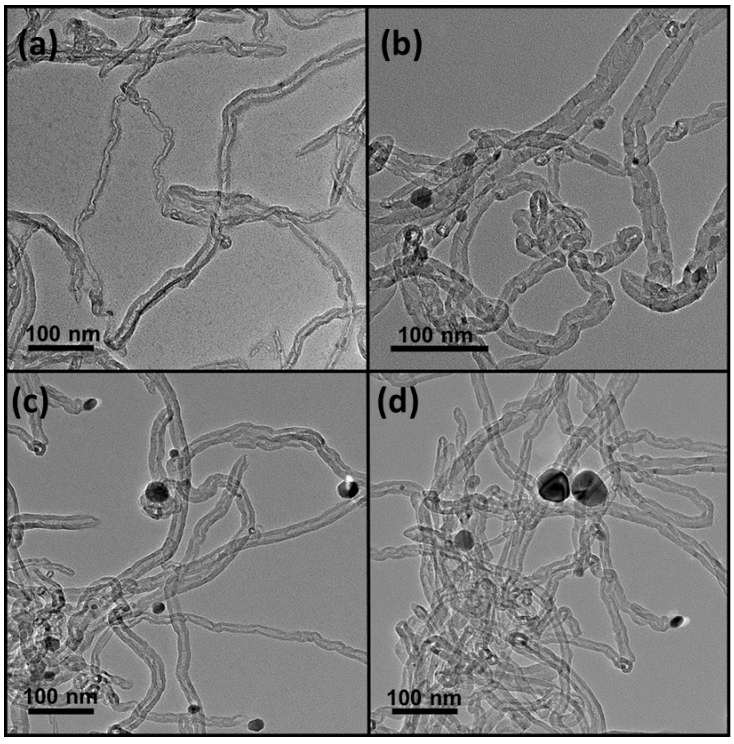

Figure 9: TEM images of the (a) bare CNTs, (b-d) Prepared Ni-Pd/CNT Catalyst.

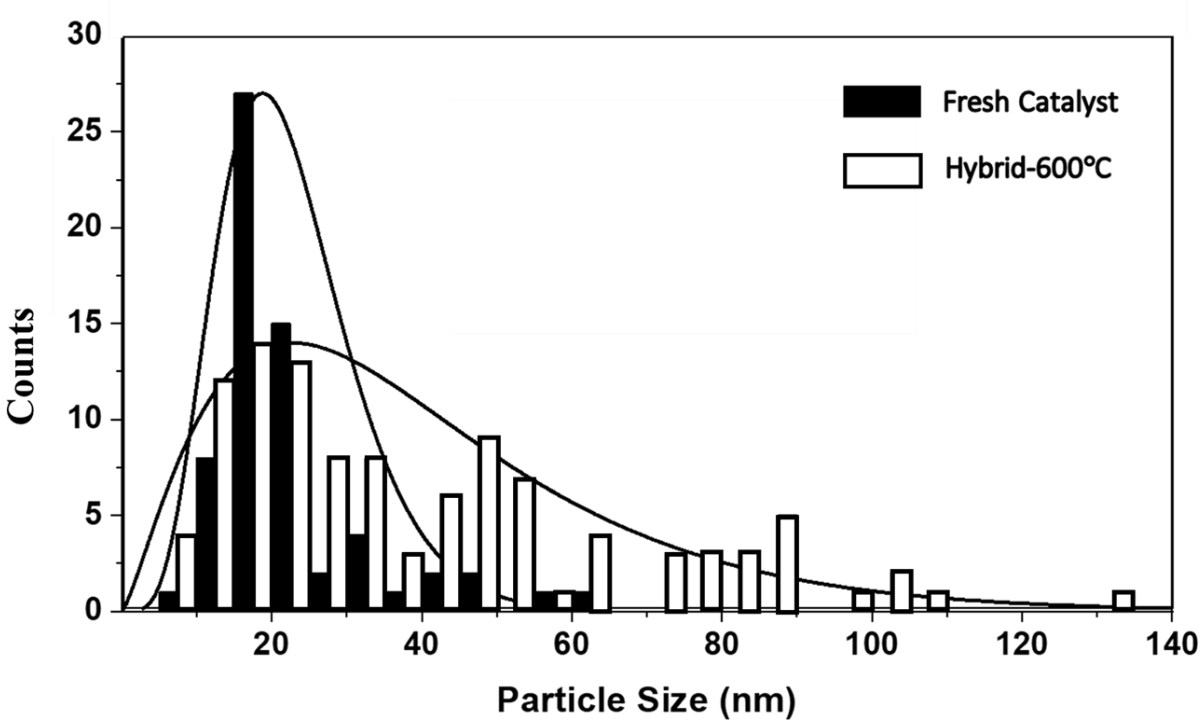

Figure 10: Histogram of metal nanoparticle size distribution in the fresh catalyst and reacted hybrid-600°C.

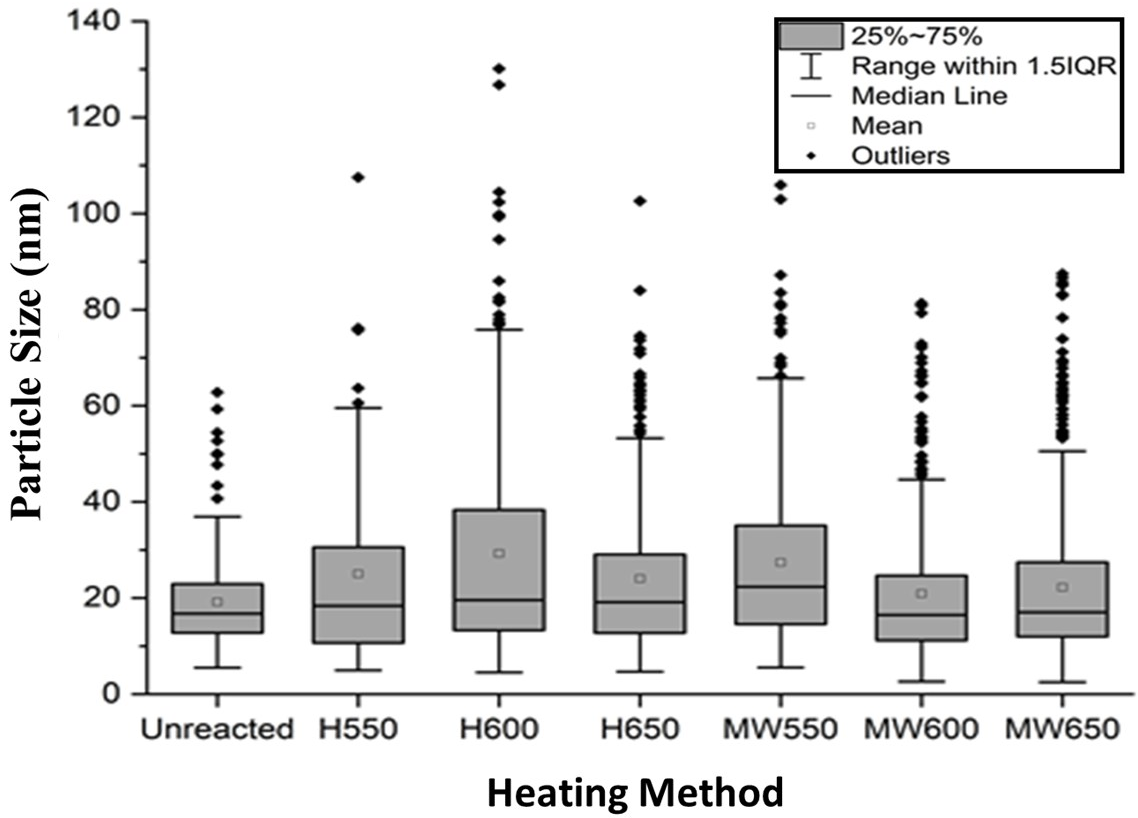

Figure 11: The particle size distribution for the microwave (MW) and the hybrid (H) heated catalysts.

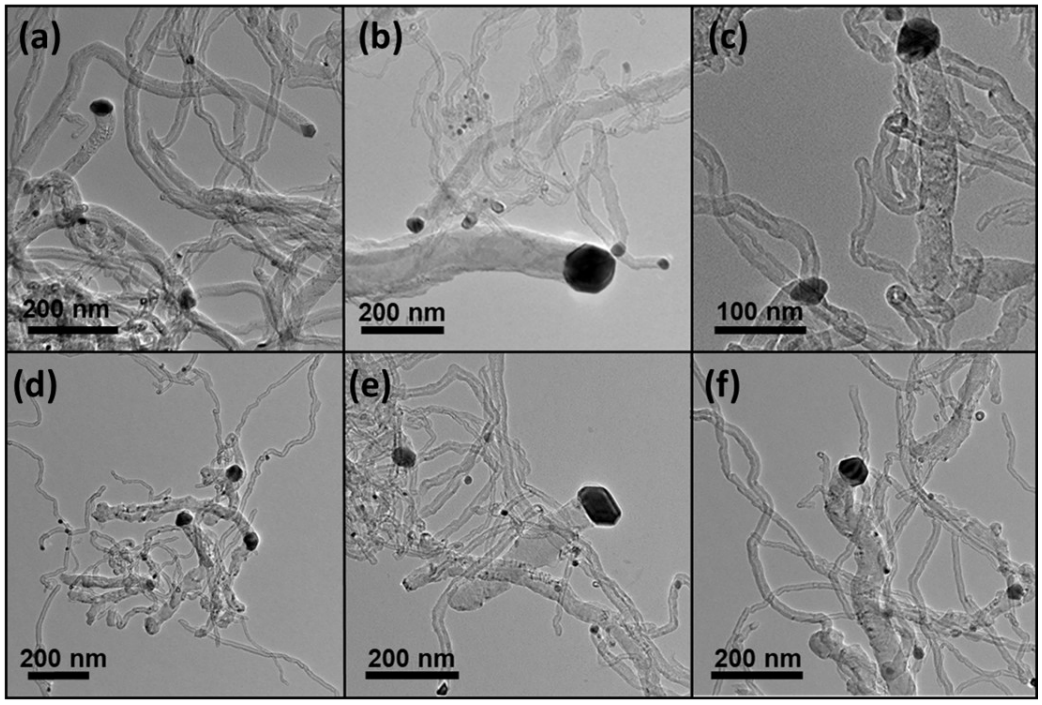

Figure 12: TEM images of (a,d) Hybrid-550°C, (b,e) Hybrid-600°C, (c,f) Hybrid-650°C

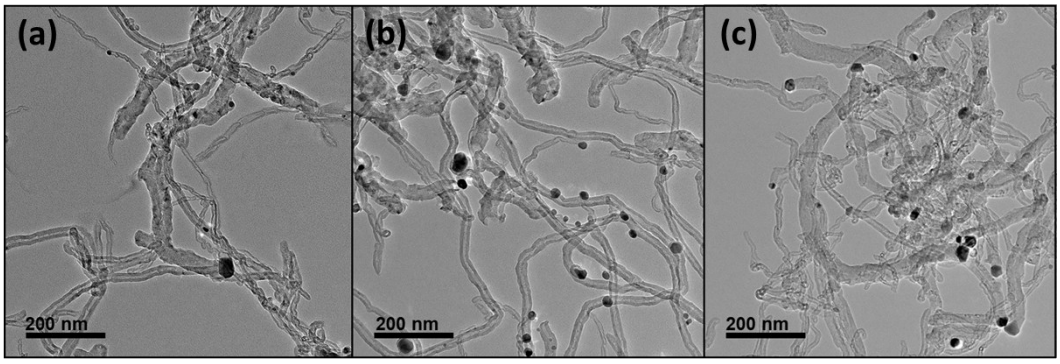

Figure 13: TEM images of (a) MW-550°C; (b) MW-600°C, (c) MW-650°C

4.0 Conclusion:

The effect of microwave radiation on thermal methane catalytic pyrolysis was tested over a CNT-Supported Ni-Pd catalyst. The catalytic activity and carbon produced were evaluated under microwave 550°C, 600°C, and 650°C temperatures and hybrid heating under 500°C of simulated waste heat at 550°C, 600°C, and 650°C temperatures. Hybrid heating was found to have a higher methane conversion than microwave heating alone for the 600°C and 650°C temperature range. The higher conversion was attributed to more efficient catalyst bed utilization and temperature uniformity, as indicated by the thermal imaging results. The conversion can be tuned in hybrid

heating mode by varying the preheating temperature or the microwave setpoint temperature. It is important to keep a sufficient temperature difference between the preheating and the microwave setpoint temperature to facilitate active hotspot generation under hybrid heating in the catalyst bed. Hybrid heating lowered the power required to facilitate the endothermic MCP reaction by over 60% of what was initially needed under microwave heating alone. Hybrid heating also was found to produce a more uniform distribution of carbon product in comparison to microwave heating alone. This work demonstrates the potential of utilizing industrial waste heat to lower the microwave reactor's overall required generator size, catalyst costs, and input energy requirements, thus reducing a microwave reactors system's overall capital cost and power requirements.

5.0 Acknowledgments:

The authors acknowledge the financial support from the National Science Foundation under award number: 2016478.

6.0 Reference:

[1] IEA, "The Future of Hydrogen," Pairs, 2019.

[2] B. Parkinson, P. Balcombe, J. F. Speirs, A. D. Hawkes, and K. Hellgardt, "Levelized cost of CO2 mitigation from hydrogen production routes," *Energy Environ. Sci.*, vol. 12, no. 1, pp. 19–40, 2019.

[3] Y. Khojasteh Salkuyeh, B. A. Saville, and H. L. MacLean, "Techno-economic analysis and life cycle assessment of hydrogen production from natural gas using current and emerging technologies," *Int. J. Hydrogen Energy*, vol. 42, no. 30, pp. 18894–18909, 2017.

[4] L. Alves, V. Pereira, T. Lagarteira, and A. Mendes, "Catalytic methane decomposition to boost the energy transition: Scientific and technological advancements," *Renew. Sustain. Energy Rev.*, vol. 137, p. 110465, 2021.

[5] Z. Fan, W. Weng, J. Zhou, D. Gu, and W. Xiao, "Catalytic decomposition of methane to produce hydrogen: A review," *J. Energy Chem.*, vol. 58, pp. 415–430, 2021.

[6] M. Msheik, S. Rodat, and S. Abanades, "Methane Cracking for Hydrogen Production: A Review of Catalytic and Molten Media Pyrolysis," *Energies*, vol. 14, no. 11, 2021.

[7] S. Schneider, S. Bajohr, F. Graf, and T. Kolb, "State of the Art of Hydrogen Production via Pyrolysis of Natural Gas," *ChemBioEng Rev.*, vol. 7, no. 5, pp. 150–158, 2020.

[8] Y. Shen and A. C. Lua, "Synthesis of Ni and Ni–Cu supported on carbon nanotubes for hydrogen and carbon production by catalytic decomposition of methane," *Appl. Catal. B Environ.*, vol. 164, pp. 61–69, 2015.

[9] H. F. Abbas and W. M. A. Wan Daud, "Hydrogen production by methane decomposition: A review," *Int. J. Hydrogen Energy*, vol. 35, no. 3, pp. 1160–1190, 2010.

[10] M. Pudukudy, Z. Yaakob, and Z. S. Akmal, "Direct decomposition of methane over Pd

promoted Ni/SBA-15 catalysts," *Appl. Surf. Sci.*, vol. 353, pp. 127–136, 2015.

[11] Y. Li, B. Zhang, X. Xie, J. Liu, Y. Xu, and W. Shen, "Novel Ni catalysts for methane decomposition to hydrogen and carbon nanofibers," *J. Catal.*, vol. 238, no. 2, pp. 412–424, 2006.

[12] U. P. M. Ashik, W. M. A. Wan Daud, and H. F. Abbas, "Production of greenhouse gas free hydrogen by thermocatalytic decomposition of methane – A review," *Renew. Sustain. Energy Rev.*, vol. 44, pp. 221–256, 2015.

[13] D. Ayillath Kutteri, I.-W. Wang, A. Samanta, L. Li, and J. Hu, "Methane decomposition to tip and base grown carbon nanotubes and COx-free H2 over mono- and bimetallic 3d transition metal catalysts," *Catal. Sci. Technol.*, vol. 8, no. 3, pp. 858–869, 2018.

[14] N. Shah, S. Ma, Y. Wang, and G. P. Huffman, "Semi-continuous hydrogen production from catalytic methane decomposition using a fluidized-bed reactor," *Int. J. Hydrogen Energy*, vol. 32, no. 15, pp. 3315–3319, 2007.

[15] I.-W. Wang *et al.*, "Catalytic decomposition of methane into hydrogen and high-value carbons: combined experimental and DFT computational study," *Catal. Sci. Technol.*, vol. 11, no. 14, pp. 4911–4921, 2021.

[16] M. A. Salam and B. Abdullah, "Catalysis mechanism of Pd-promoted γ-alumina in the thermal decomposition of methane to hydrogen: A density functional theory study," *Mater. Chem. Phys.*, vol. 188, pp. 18–23, 2017.

[17] C. Jiang *et al.*, "Methane Catalytic Pyrolysis by Microwave and Thermal Heating over Carbon Nanotube-Supported Catalysts: Productivity, Kinetics, and Energy Efficiency," *Ind. \& Eng. Chem. Res.*, vol. 61, no. 15, pp. 5080–5092, 2022.

[18] Z. Ye, W. D. Deering, A. Krokhin, and J. A. Roberts, "Microwave absorption by an array of carbon nanotubes: A phenomenological model," *Phys. Rev. B*, vol. 74, no. 7, p. 75425, Aug. 2006.

[19] M. Xu *et al.*, "Structure sensitivity and its effect on methane turnover and carbon co-product selectivity in thermocatalytic decomposition of methane over supported Ni catalysts," *Appl. Catal. A Gen.*, vol. 611, p. 117967, 2021.

[20] M. Mohiuddin and S. V Hoa, "Temperature dependent electrical conductivity of CNT–PEEK composites," *Compos. Sci. Technol.*, vol. 72, no. 1, pp. 21–27, 2011.

[21] A. Aqel, K. M. M. A. El-Nour, R. A. A. Ammar, and A. Al-Warthan, "Carbon nanotubes, science and technology part (I) structure, synthesis and characterisation," *Arab. J. Chem.*, vol. 5, no. 1, pp. 1–23, 2012.

[22] H. Wang, X. Kou, J. Zhang, and J. Li, "Large scale synthesis and characterization of Ni nanoparticles by solution reduction method," *Bull. Mater. Sci.*, vol. 31, no. 1, pp. 97–100, 2008.

[23] R. Bhaskar, J. Li, and L. Xu, "A Comparative Study of Particle Size Dependency of IR and XRD Methods for Quartz Analysis," *Am. Ind. Hyg. Assoc. J.*, vol. 55, no. 7, pp. 605–609, 1994.

[24] S. A. Hooker, R. Geiss, R. Schilt, and A. Kar, "Rapid Inspection of Carbon Nanotube Quality," *Nanostructured Mater. Nanotechnol.*, pp. 119–130, 2009.

[25] L. Bokobza, J.-L. Bruneel, and M. Couzi, "Raman Spectra of Carbon-Based Materials (from Graphite to Carbon Black) and of Some Silicone Composites," *C*, vol. 1, no. 1, pp. 77–94, 2015.

[26] A. Gohier, C. P. Ewels, T. M. Minea, and M. A. Djouadi, "Carbon nanotube growth mechanism switches from tip- to base-growth with decreasing catalyst particle size," *Carbon N. Y.*, vol. 46, no. 10, pp. 1331–1338, 2008.

Graphical Abstract: